Electronic Research Archive

https://www.aimspress.com/journal/era

ERA, 34(4): 2590–2606.
DOI: 10.3934/era.2026120
Received: 06 January 2026
Revised: 17 February 2026
Accepted: 12 March 2026
Published: 24 March 2026

Research article

Sliding mode control for impulsive electrohydraulic position servo systems with external disturbances

Mingzhong Li, Zhen Fu, Shuai Liu* and Jianbing Wang

Beijing Tianma Intelligent Control Technology Co., Ltd., Beijing 101399, China

* **Correspondence:** Email: liushuai@tdmarco.com.

Abstract: This paper studied the trajectory tracking performance of electrohydraulic position servo systems subject to impulsive disturbance via sliding mode control. Different from traditional sliding mode control, which in applied in continuous state space, our proposed sliding mode control could restrain the negative effect of impulsive disturbance. The proposed method is based on the linear matrix inequality method; some sufficient conditions were presented to ensure the reachability of the sliding surface and the stability of the resulting sliding mode dynamics, where a relationship between continuous dynamics, impulsive strength, and impulsive frequency was established. It showed that this relationship can fully estimate the effect of impulsive disturbance. Moreover, we provided the estimation of the reaching time, which was related to the impulse actions and initial state. Finally, the simulations demonstrated the validity of the obtained results.

Keywords: electrohydraulic position servo system; impulsive disturbance; linear matrix inequality; reaching time; sliding mode control

1. Introduction

Impulsive systems, as a special subclass of hybrid systems, consist of three main components: continuous dynamics governed by ordinary differential equations, discrete dynamics subject to instantaneous state jumps, and impulsive law that determines when impulses occur. Generally, impulsive systems serve as fundamental mathematical models for describing complex physical phenomena involving sudden changes, such as epidemic models in pathology [1], spacecraft relative motions [2], and electronic networks [3]. Over the past decades, the study of impulsive systems has attracted increasing attention; see [4–7] and the references therein. Based on these results, one may observe that the study of impulsive systems includes two types. One type of study focuses on the case where a system without impulse cannot exhibit desired properties (such as boundness and stability), and such performances can be achieved via admissible impulsive actions, called the impulse control

problem. Because impulsive control has significant advantages of simple structure and low energy consumption, it has been applied in various practical scenarios, including network synchronization, secure communication, and satellite rendezvous [8–10]. Another type of study focuses on the case in which a system exhibits some properties in absence of impulse, and moreover, these performances can be maintained even when the system subject to instantaneous disturbance, known as the impulsive disturbance problem. So far, an increasing number of results on the impulsive disturbance problem have been reported in the literature; see [11, 12].

Electrohydraulic position servo systems are commonly used as basic models for imitating dynamical processes of force loading and performing structural static tests [13]. Because electrohydraulic position servo systems can effectively realize a higher force-to-weight ratio, faster response speed, and better position capabilities than other systems, they have been extensively applied in many fields, such as aerospace explorations [14], vehicle suspension systems [15], ship steering gear [16], and especially coal mining machinery [17]. Recently, there have been many typical advanced control methods on the precision tracking of electrohydraulic position servo systems; see [18–29]. In particular, studies [18, 19] designed proportional integral derivative controllers for trajectory tracking problems of electrohydraulic position servo systems, where some restrictions on the regulation of control parameters were imposed, resulting in lower tracking precision. Preset performance control was investigated in [20], where a homeomorphic transformation and performance functions were designed to constrain the bound of trajectory tracking errors. Study [21] proposed a novel prescribed performance fault-tolerant control method for electrohydraulic servo systems with actuator faults, external disturbances, and unknown nonlinearities. However, the above results [20, 21] only ensure that the trajectory tracking errors remain within the prescribed bounds. To improve the tracking performance, study [22] designed an appropriate backstepping controller to stabilize the electrohydraulic position servo systems in a strict-feedback form. In [23], the stability of an electrohydraulic servo system was studied by designing model predictive control regulator. It is worth noting that the backstepping method in [22] requires repeated calculation of the derivative of the virtual control law, and the method in [23] involves solving online optimization problems and relies on an accurate prediction model, which increases the complexity of both the analysis and design. To reduce the computational burden, studies [24, 25] investigated the stabilization problems for electrohydraulic force servo systems via adaptive control, where the parametric uncertainties were primarily addressed. However, the adaptive control in [24, 25] exhibited limited robustness against external disturbances. Subsequently, neural network compensators were developed in [26, 27], and an observer-based event-triggered control method was provided in [28] to estimate external disturbances. Although such methods can effectively attenuate disturbances, the control performance strongly relies on the accuracy of disturbance estimation or learning processes. By contrast, sliding mode control (SMC) guarantees strong robustness to external disturbances and uncertainties, including friction, bulk modulus variation, and leakage of the hydraulic cylinder of electrohydraulic position servo systems [29]. More specifically, SMC ensures that the trajectory can reach a sliding surface in finite time and then tend to the origin along such a surface. Up to date, SMC has attracted considerable research attention in the literature [30–34]. Especially, based on the linear matrix inequality method, fuzzy fast terminal SMC was proposed in [31] for multi-input, multi-output systems to achieve finite-time convergence of the system trajectories. However, such a method was developed under the assumption of fault-free actuators. To enhance robustness in the presence of

actuator faults, an adaptive-barrier global SMC was investigated in [32] for uncertain systems with faulty actuators, where external disturbances are assumed to be bounded. To relax such restrictions on external disturbances, the barrier function adaptive technique was employed in [34] to estimate the unknown upper bounds of external disturbances.

It worth noting that there have been more and more interesting works on SMC for electrohydraulic position servo systems, see [35–38]. For example, study [35] designed a high-order sliding mode control with varying boundary layers, which only ensures the bounded tracking performance of electrohydraulic position servo systems, thereby limiting the application ranges. Recently, adaptive SMC was proposed in [36] to identify parameter uncertainties and deal with external disturbances. However, when the systems are subject to impulsive disturbance, the existing results using SMC for these systems, such as [35–38], are infeasible. In fact, when the system involves impulsive disturbance, it is challenging to estimate the reaching time of the sliding surface. Moreover, it remains unknown whether the sliding mode dynamics could be avoided from jumping off the sliding surface, which further increases analysis complexity to some extent.

Inspired by the discussion above, this article studies the trajectory tracking performance for impulsive electrohydraulic position servo systems via SMC. We present some sufficient conditions to guarantee the reachability of the sliding surface and achieve the stability of sliding mode dynamics. The innovations of this paper are outlined.

(i) SMC is proposed for the trajectory tracking performance of electrohydraulic position servo systems with external disturbance. Compared with the existing typical control methods [24–28], the proposed SMC guarantees strong robustness to external disturbances.

(ii) A relationship between continuous dynamics, impulsive strength, and impulsive frequency is established in this paper to fully estimate the effect of impulsive disturbance. Unlike traditional SMC [30–38], which was applied in continuous state space, our proposed SMC could restrain the negative effect of impulsive disturbance.

(iii) There is no need to impose a uniformly bounded assumption on the intervals between two consecutive impulse signals. Compared with integral SMC [39], the proposed method allows the impulse signals to be flexibly regulated.

This article is divided into five sections, organized as follows. The dynamic models of electrohydraulic position servo systems and some preliminary results are provided in Section 2. In Section 3, some sufficient conditions for the reachability of the sliding surface and the stability of the resulting sliding mode dynamics are established. Some simulations are conducted to validate the obtained results in Section 4. Section 5 gives some conclusions.

Notations. The set of real numbers is denoted by $\mathbb{R}$. Let $\mathbb{R}_+ = \{a \in \mathbb{R} : a \geq 0\}$. $\mathbb{Z}_+$ represents the set of positive integers. $\mathbb{R}^n$ stands for the n-dimensional Euclidean space. Denote as $\lambda_{\max}(A)$ ($\lambda_{\min}(A)$) the maximum (minimum) eigenvalue of matrix A. For two constants m and n, $m \wedge n$ stands for the minimum value.

2. Dynamic models and preliminaries

2.1. Dynamic models of electrohydraulic position servo systems

The electrohydraulic position servo systems consist of a double-rod hydraulic cylinder, a three-position four-way servo valve, and an external load with disturbances [36]. Note that the working principle of the electrohydraulic position servo systems is that the servo valve regulates the hydraulic fluid flow to drive the cylinder, thereby powering the external load, as shown in Figure 1. The dynamic models of the electrohydraulic position servo systems can be described by the following three equations. Consider the flow equation of the servo valve,

$$Q_L = K_q y_v - K_c P_L, \tag{2.1}$$

in which K_c is the pressure coefficient, K_q is gain, Q_L is the load flow, and $P_L = P_1 - P_2$ is the load pressure. P_1 and P_2 are the pressures of two chambers, respectively. $y_v = K_a u$ represents the servo-valve spool displacement, where K_a is the servo amplifier gain, and u is the control voltage [40]. Moreover, based on the flow conservation law, the flow pressure continuous equation is given by

$$Q_L = A\dot{y} + \frac{1}{4\beta_e} V_t \dot{P}_L + C_{te} P_L, \tag{2.2}$$

where y is the piston position, and $\dot{y}$ is the upper right-hand derivative of y. A is the effective area, V_t is the total volume, and C_{te} is the total leakage coefficient of the hydraulic cylinder. β_e denotes the effective fluid bulk modulus. The force balance equation can be derived as follows:

$$AP_L = M\ddot{y} + B_c\dot{y} + K_s y + F_L, \tag{2.3}$$

where M is the load mass, K_s is the stiffness coefficient, B_c is the damping coefficient, and F_L is the external load.

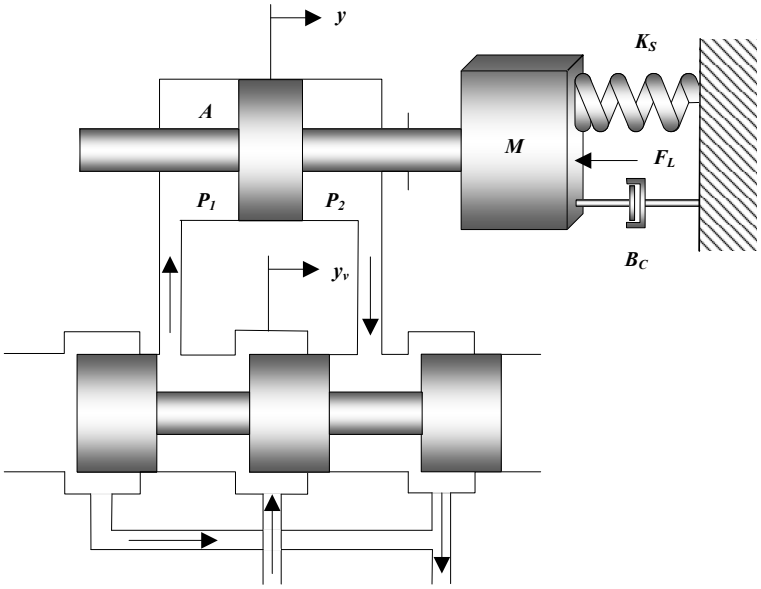

Figure 1. Schematic drawing of an electrohydraulic position servo system.

2.2. Preliminaries

Let $x = [x_1, x_2, x_3]^T = [y, \dot{y}, \ddot{y}]^T$. Combining with (2.1)–(2.3), the state space equation of the electrohydraulic position servo systems can be expressed as

$$\begin{cases} \dot{x}_1(t) = x_2(t) \\ \dot{x}_2(t) = x_3(t) \\ \dot{x}_3(t) = a_1 x_1(t) + a_2 x_2(t) + a_3 x_3(t) + d(t) + bU(t),\ t \geq 0, \end{cases} \tag{2.4}$$

where

$$a_1 = -\frac{1}{M}K_s\beta,\ a_2 = -\frac{1}{M}\left(K_s + B_c\beta + A^2\alpha\right),\ a_3 = -\frac{1}{M}B_c - \beta,$$
$$d(t) = -\frac{1}{M}\left(\dot{F}_L + \beta F_L\right),\ b = \frac{1}{M}\alpha A K_q K_a,\ \alpha = \frac{4\beta_e}{V_t},\ \beta = \alpha(C_{te} + K_c).$$

In practice, due to the noise, uncertainties and unexpected obstructions, the electrohydraulic position servo systems may be subject to instantaneous disturbance, which exhibits sudden changes in state variables x_2 and x_3 at certain instants, that is, impulsive disturbance. One then considers impulsive disturbance as follows:

$$\Delta x(t) = Gx(t^-),\ t = t_k \tag{2.5}$$

with

$$G = \begin{pmatrix} 0 & 0 & 0 \\ 0 & g_2 & g_3 \\ 0 & g_4 & g_5 \end{pmatrix},$$

and $g_i \in \mathbb{R}$ for $i = 2, 3, 4, 5$. $x(t^-)$ stands for the left limit, and $\Delta x(t) := x(t) - x(t^-)$ represents the state jump at impulse instants. The sequence $\{t_k : k \in \mathbb{Z}_+\}$ (short for $\{t_k\}$) denotes the impulse time sequence satisfying $0 = t_0 < t_1 < \cdots < t_k \to \infty$ as $k \to \infty$. Define such a class of $\{t_k\}$ by set $\mathcal{S}$. In this paper, all signals are supposed to be right-continuous.

Consider the slave impulsive electrohydraulic position servo systems (2.4)–(2.5) and the master impulsive electrohydraulic position servo system which can be described as

$$\begin{cases} \dot{x}_{d1}(t) = x_{d2}(t) \\ \dot{x}_{d2}(t) = x_{d3}(t) \\ \dot{x}_{d3}(t) = a_1 x_{d1}(t) + a_2 x_{d2}(t) + a_3 x_{d3}(t),\ t \neq t_k, \\ \Delta x_d(t_k) = G x_d(t_k^-) \end{cases} \tag{2.6}$$

with $x_d = [x_{d1}, x_{d2}, x_{d3}]^T$. Define the tracking error as $e = x - x_d = [e_1, e_2, e_3]^T$, so that the error system can be written as

$$\begin{cases} \dot{e}_1(t) = e_2(t) \\ \dot{e}_2(t) = e_3(t) \\ \dot{e}_3(t) = a_1 e_1(t) + a_2 e_2(t) + a_3 e_3(t) + d(t) + bU(t),\ t \neq t_k, \\ e(t_k) = \bar{G} e(t_k^-), \end{cases} \tag{2.7}$$

where matrix $\bar{G} = I+G$. For any given $\{t_k\} \in \mathcal{S}$, suppose that $e(t) = e(t, 0, e_0, \{t_k\})$ stands for the solution of error system (2.7), with the initial state $e_0 \in \mathbb{R}^3$. This paper aims to ensure that error system (2.7) can exponentially converge to the origin by designing the input voltage of SMC.

Assumption 2.1. The external disturbance $d(t)$ is bounded with $|d(t)| \leq \bar{d}$ for all $t \geq 0$, where $\bar{d}$ is a positive constant.

Assumption 2.2. There exist some constants c_1, c_2, and $\mu \geq 1$ such that

$$\bar{G}^T C^T C \bar{G} \leq \mu^2 C^T C, \tag{2.8}$$

where matrix $C = [c_1\ c_2\ 1]$.

3. Main results

In this section, we establish some sufficient conditions to guarantee that error system (2.7) can reach a sliding surface and exponentially converges to equilibrium along such surface.

To begin, we construct the following sliding surface and SMC:

$$\Gamma(t) = c_1 e_1(t) + c_2 e_2(t) + e_3(t) = Ce(t) = 0,$$
$$U(t) = -\frac{1}{b}(a_1 e_1(t) + (c_1 + a_2)e_2(t) + (c_2 + a_3)e_3(t) + \eta sign(\Gamma(t))), \tag{3.1}$$

where control gain $\eta > \bar{d}$. For any given $\mu \geq 1$, define by $\mathcal{S}_1$ the class of $\{t_k\}$ in $\mathcal{S}$ satisfying

$$\min\left\{i \in \mathbb{Z}_+ : \frac{t_i}{\mu^{i-1}} \geq \frac{\sigma}{\eta - \bar{d}}\right\} := N < +\infty. \tag{3.2}$$

Let $\Omega_\sigma = \{z \in \mathbb{R}^3 : |Cz| \leq \sigma\}$, where $\sigma > 0$.

Theorem 3.1. Under Assumptions 1–2, the states of error system (2.7) with $e_0 \in \Omega_\sigma$ under SMC in (3.1) over the class $\mathcal{S}_1$ can reach $\Gamma(t) = 0$ in finite time, which can be estimated by

$$T(e_0, \{t_k\}) \leq \frac{\mu^{N-1}\sigma}{\eta - \bar{d}},\ \forall e_0 \in \Omega_\sigma,\ \{t_k\} \in \mathcal{S}_1. \tag{3.3}$$

Proof. For given $e_0 \in \Omega_\sigma$, suppose that $e(t) = e(t, 0, e_0, \{t_k\})$ stands for the solution of error system (2.7). Define $\mathcal{V}(t) = 1/2\Gamma^T(t)\Gamma(t)$. When $t = t_k$, for all $k \in \mathbb{Z}_+$, it can be obtained from (2.8) that

$$\mathcal{V}(t_k) = \frac{1}{2}e^T(t_k)C^T Ce(t_k) = \frac{1}{2}e^T(t_k^-)\bar{G}^T C^T C\bar{G}e(t_k^-) \leq \mu^2 \mathcal{V}(t_k^-). \tag{3.4}$$

When $t \in [t_{k-1}, t_k)$, calculating the right-upper Dini derivative of $\mathcal{V}(t)$ along the solution of error system (2.7), we obtain

$$\begin{aligned} D^+\mathcal{V}(t) &= \Gamma^T(t)\left(c_1 e_2(t) + c_2 e_3(t) + a_1 e_1(t) + a_2 e_2(t) + a_3 e_3(t) + bU(t) + d(t)\right) \\ &\leq -(\eta - \bar{d})|\Gamma(t)| \\ &\leq -\sqrt{2}(\eta - \bar{d})\mathcal{V}^{\frac{1}{2}}(t). \end{aligned} \tag{3.5}$$

Next, we shall claim that error system (2.7) with $e_0 \in \Omega_\sigma$ over the class $\mathcal{S}_1$ can reach $\Gamma(t) = 0$ in finite time. Denote $\delta := \eta - \bar{d} > 0$ and $\xi = \sigma/\delta$. One derives from (3.5) that for all $t \in [0, t_1 \wedge \xi)$,

$$\mathcal{V}^{\frac{1}{2}}(t) \leq \mathcal{V}^{\frac{1}{2}}(0) - \frac{\sqrt{2}}{2}\delta t. \tag{3.6}$$

Then, we shall consider two possible cases, namely, $t_1 \geq \xi$ and $t_1 < \xi$. When $t_1 \geq \xi$, that is, $N = 1$, one gets $\Gamma(t) \equiv 0$ for $t \geq \xi$. Otherwise $t_1 < \xi$, we have $N \geq 2$. By (3.5)–(3.6), one derives that for all $t \in [t_1, t_2 \wedge \mu\xi)$,

$$\begin{aligned}
\mathcal{V}^{\frac{1}{2}}(t) &\leq \mu\mathcal{V}^{\frac{1}{2}}(t_1^-) - \frac{\sqrt{2}}{2}\delta(t - t_1) \\
&\leq \mu\left(\mathcal{V}^{\frac{1}{2}}(0) - \frac{\sqrt{2}}{2}\delta t_1\right) - \frac{\sqrt{2}}{2}\delta(t - t_1) \\
&\leq \mu\frac{\sqrt{2}}{2}\delta - \frac{\sqrt{2}}{2}\delta t.
\end{aligned}$$

Similar to the above discussion, when $t_2 \geq \mu\xi$, we have $\Gamma(t) \equiv 0$ for all $t \geq \mu\xi$. Otherwise $t_2 < \mu\xi$, it implies that $N \geq 3$. In view of the definition of N in (3.2), one derives that $t_i < \mu^{i-1}\xi$ for all $i = 1, 2, \ldots, N-1$ and $t_N > \mu^{N-1}\xi$. Then one obtains for $t \in [t_{N-1}, \mu^{N-1}\xi)$,

$$\mathcal{V}^{\frac{1}{2}}(t) \leq \mu^{N-1}\frac{\sqrt{2}}{2}\delta - \frac{\sqrt{2}}{2}\delta t,$$

and $\Gamma(t) \equiv 0$ for all $t \geq \mu^{N-1}\xi$. Hence, the solution of error system (2.7) with $e_0 \in \Omega_\sigma$ under SMC in (3.1) over the class $\mathcal{S}_1$ can reach $\Gamma(t) = 0$, where the reaching time can be estimated by (3.3). This completes the proof. □

Remark 3.1. Theorem 1 presents some sufficient conditions to guarantee the reachability of the sliding surface $\Gamma(t) = 0$ for error system (2.7) via SMC in (3.1), which involves a *sign* function. Then, substituting SMC in (3.1) into error system (2.7) results in a system with a discontinuous property. Thus, the system states are understood in the Filippov's sense [41].

Remark 3.2. Note that traditional SMC guarantees the state of the systems continuously reach $\Gamma(t) = 0$ in finite time. When the impulsive disturbance is involved, it is possible that the state trajectory becomes discontinuous. In this case, the existing results on traditional *SMC*, such as those in [30–38], are no longer applicable. Different from the above results, the SMC in (3.1) and the class $\mathcal{S}_1$ of $\{t_k\}$ satisfying condition (3.2) are proposed to ensure the reachability of the sliding surface $\Gamma(t) = 0$. It is worth noting that condition (3.2) establishes a relationship between continuous dynamics, impulsive strength, and impulsive frequency to fully extract the information of impulsive disturbance. In addition, under such impulse effects, note that the reaching time $T(e_0, \{t_k\})$ in (3.3) depends not only on the initial state e_0 but also on the class $\mathcal{S}_1$. Compared with traditional SMC, where reaching time is estimated by $\sigma/(\eta - \bar{d})$, the negative effect of impulsive disturbance leads to a larger bound of $T(e_0, \{t_k\})$.

By Theorem 1, when the solution of error system (2.7) slides on $\Gamma(t) = 0$, it yields that

$$e_3(t) = -c_1 e_1(t) - c_2 e_2(t). \tag{3.7}$$

By substituting (3.7) into error system (2.7), sliding mode dynamics can be obtained:

$$\begin{cases} \dot{\chi}(t) = A_0\chi(t),\ t \neq t_k, \\ \chi(t) = \bar{G}_0\chi(t^-),\ t = t_k,\ t \geq T_0, \end{cases} \tag{3.8}$$

where

$$\chi = \begin{pmatrix} e_1 \\ e_2 \end{pmatrix},\ A_0 = \begin{pmatrix} 0 & 1 \\ -c_1 & -c_2 \end{pmatrix},\ \bar{G}_0 = \begin{pmatrix} 1 & 0 \\ -c_1 g_3 & 1 + g_2 - c_2 g_3 \end{pmatrix},\ T_0 = T(e_0, \{t_k\}),$$

satisfying that A_0 is Hurwitz. Denote by $\mathcal{S}_2$ the class of $\{t_k\}$ in $\mathcal{S}_1$ satisfying for all $t \geq T_0 \geq 0$,

$$\mathcal{N}(T_0, t) \leq \frac{t - T_0}{\tau} + \bar{N}, \tag{3.9}$$

where $\mathcal{N}(T_0, t)$ is the count of impulses on $(T_0, t]$ and τ, $\bar{N}$ are positive constants.

Theorem 3.2. Under Assumptions 1–2, if there exist constants $\lambda, \mu_1 \geq 1$, and matrix $\mathcal{P} > 0$ such that

$$\mathcal{P}A_0 + A_0^T\mathcal{P} \leq -\lambda\mathcal{P}, \tag{3.10}$$

$$\bar{G}_0^T\mathcal{P}\bar{G}_0 \leq \mu_1\mathcal{P}, \tag{3.11}$$

then the states of error system (2.7) with $e_0 \in \Omega_\sigma$ under *SMC* in (3.1) can exponentially converge to the origin over the class $\mathcal{S}_2$, with τ satisfying

$$\tau > \frac{\ln \mu_1}{\lambda}. \tag{3.12}$$

Proof. By Theorem 1, the solution of error system (2.7) under SMC in (3.1) can reach $\Gamma(t) = 0$. In the following, we consider sliding mode dynamics (3.8). Let $\mathcal{V}_1(t) = \chi^T(t)P\chi(t)$. Without loss of generality, when the solution of error system (2.7) reaches $\Gamma(t) = 0$, suppose that $t_m > T_0$ is the instant at which the first impulse occurs, where $m \in \mathbb{Z}_+$. When $t \neq t_{m+j-1}$ for all $j \in \mathbb{Z}_+$, along the solution of sliding mode dynamics (3.8), it can be derived from condition (3.10) that for $t \geq T_0$,

$$D^+\mathcal{V}_1(t) \leq -\lambda\chi^T(t)\mathcal{P}\chi(t) = -\lambda\mathcal{V}_1(t). \tag{3.13}$$

When $t = t_{m+j-1}$ for all $i \in \mathbb{Z}_+$, by condition (3.11), it holds that

$$\begin{aligned} \mathcal{V}_1(t_{m+j-1}) = \chi^T(t_{m+j-1})\mathcal{P}\chi(t_{m+j-1}) &= \chi^T(t_{m+j-1}^-)\bar{G}_0^T\mathcal{P}\bar{G}_0\chi(t_{m+j-1}^-) \\ &\leq \mu_1\chi^T(t_{m+j-1}^-)\mathcal{P}\chi(t_{m+j-1}^-) = \mu_1\mathcal{V}_1(t_{m+j-1}^-). \end{aligned} \tag{3.14}$$

When $t \in [T_0, t_m)$, it holds that

$$\mathcal{V}_1(t) \leq \exp(-\lambda(t - T_0))\mathcal{V}_1(T_0). \tag{3.15}$$

When $t \in [t_{m+j-1}, t_{m+j})$ for all $i \in \mathbb{Z}_+$, it can be deduced from (3.13) and (3.14) that

$$\mathcal{V}_1(t) \leq \exp(-\lambda(t - t_{m+j-1}))\mathcal{V}_1(t_{m+j-1})$$

$$\begin{aligned}
&\leq \mu_1 \exp(-\lambda(t - t_{m+j-1}))\mathcal{V}_1(t^-_{m+j-1}) \\
&\leq \mu_1 \exp(-\lambda(t - t_{m+j-2}))\mathcal{V}_1(t_{m+j-2}) \\
&\cdots \\
&\leq \mu_1^{\mathcal{N}(T_0,t)} \exp(-\lambda(t - T_0))\mathcal{V}_1(T_0). \qquad (3.16)
\end{aligned}$$

By (3.12), (3.15), and (3.16), one has that for $t \geq T_0$,

$$\mathcal{V}_1(t) \leq \exp\left(\bar{N}\ln\mu_1 + \left(\frac{\ln\mu_1}{\tau} - \lambda\right)(t - T_0)\right)\mathcal{V}_1(T_0),$$

which means that

$$|\chi(t)| \leq \gamma \exp(-\theta(t - T_0))|\chi(T_0)|, \ \forall t \geq T_0,$$

where $\gamma = \left(\lambda_{\max}(\mathcal{P})\exp(\bar{N}\ln\mu_1)/\lambda_{\min}(\mathcal{P})\right)^{1/2}$, and $\theta = 1/2(\lambda - \ln\mu_1/\tau)$. Thus, sliding mode dynamics (3.8) are exponentially stable, indicating that the state of error system (2.7) with $e_0 \in \Omega_\sigma$ can exponentially converge to the origin. The proof is complete. □

Remark 3.3. Theorem 2 presents linear matrix inequalities-based conditions (3.10) and (3.11) for the stability of sliding mode dynamics (3.8), involving the unknown terms λ and μ_1. In implementation, we first design term λ, which describes the possible convergence rate of continuous dynamics. It can be derived from condition (3.10) that the larger λ is, the closer $\lambda\mathcal{P}$ approximates $\mathcal{P}A_0 + A_0^T\mathcal{P}$. The term λ can be derived by the maximization problem as follows:

$$\begin{cases} \text{Maximum } \lambda, \\ \text{Linear matrix inequality in (3.10).} \end{cases}$$

One may obtain the feasible solution of matrix $\mathcal{P}$ accordingly. In view of the feasible solution $\mathcal{P}$, it follows from condition (3.11) that it is desirable to find the minimum μ_1, where μ_1 describes the possible impulsive strength. Specifically, the terms λ and μ_1 can be selected by the following step-by-step algorithmic implementation procedures.

Algorithm 3.1.

Step 1: Given positive constants $\mu_1 = 1$, $\lambda > 0$, step length $\iota > 0$, and matrix C.
Step 2: Check (3.10). If (3.10) is satisfied, then increase λ by a step size of ι until (3.10) infeasible. Set $\lambda = \lambda - \iota$ to return to the last feasible solution. Otherwise, decrease $\lambda > 0$ by a step size of ι until (3.10) first holds.
Step 3: Solve (3.10) to obtain $\mathcal{P}$ using λ from *Step 2*.
Step 4: Check (3.11) using $\mathcal{P}$ from *Step 3*. If (3.11) is satisfied, then go to *Step 5*. Otherwise, increase μ_1 by a step size of ι until (3.11) holds.
Step 5: Output μ_1, λ and $\mathcal{P}$. Stop.

Remark 3.4. Study [39] studied the stabilization of impulsive systems via SMC. To deal with the impulsive disturbance, a term involving the impulse effects was specially introduced into the sliding

functions in [39]. Unlike the above result, our proposed SMC adopts the linear sliding function, leading to easy-to-verify SMC laws that facilitate implementation. On the other hand, study [39] provided a uniformly bounded assumption on the intervals between two consecutive impulse signals, namely, $\sigma_0 \leq t_k - t_{k-1} \leq \sigma_1$ with $0 < \sigma_0 \leq \sigma_1$, for all $k \in \mathbb{Z}_+$. In fact, the above assumption reduced the rationality and flexibility of impulse time sequences to a certain extent. In this paper, however, the restriction on the bound of impulse time sequences is dropped. More specifically, the first N impulse signals can be flexibly regulated based on condition (3.2) in Theorem 1. Based on the average dwell-time approach, it can be seen from condition (3.12) in Theorem 2 that the restriction on sequence $\{t_k\}$ has been relaxed.

4. Simulations

In this section, we provide some simulations to validate the proposed approach.

Table 1. Parameters for system (2.4).

Parameter	Meaning	Numerical value	Unit
M	Load mass	30	kg
B_c	Damping coefficient	1500	N·s/m
K_s	Stiffness coefficient	4×10^4	N/m
A	Effective area	4.71×10^{-4}	m^2
K_q	Gain	0.05	m^2/s
K_a	Servo amplifier gain	2×10^{-4}	m/V
V_t	Total volume	1.88×10^{-4}	m^3
β_e	Effective fluid bulk modulus	6.9×10^8	Pa
C_{te}	Total leakage coefficient	1.55×10^{-12}	$m^3/(s \cdot Pa)$
K_c	Pressure coefficient	1.12×10^{-11}	$m^3/(s \cdot Pa)$
F_L	External load	$50\sin(\pi t)$	N

Consider System (2.4) with parameters shown in Table 1. In reality, due to the rough ground, System (2.4) is subjected to discontinuous disturbance. Such disturbance is regarded as impulsive disturbance in the form of

$$\Delta x(t_k) = Gx(t_k^-) = \begin{pmatrix} 0 & 0 & 0 \\ 0 & 1 & -5 \\ 0 & -0.1 & 0.5 \end{pmatrix} x(t_k),$$

which indicates that x_2 and x_3 are subjected to sudden changes. According to Assumption 1, we derive that $\bar{d} = 312.0121$. Choose $C = [0.1\ 0.1\ 1]$ such that A_0 is a Hurwitz matrix. Then, we obtain that

$$\Gamma(t) = 0.1e_1(t) + 0.1e_2(t) + e_3(t) = 0.$$

Let control gain $\eta = 313 > \bar{d}$, and $U(t)$ is obtained as follows:

$$U(t) = 108.2803e_1(t) + 51.7389e_2(t) + 0.1029e_3(t) - 0.1358sign(\Gamma(t)). \tag{4.1}$$

According to Assumption 2, it is desirable to find the minimum $\mu = 1$. By Theorem 1, we conclude that the states of error system (2.7) with $e_0 \in \Omega_\sigma$ under SMC in (4.1) over the class $\mathcal{S}_1$ can reach $\Gamma(t) = 0$, where $\mathcal{S}_1 \subseteq \mathcal{S}$ respects the class of $\{t_k\}$, which meets

$$\min\left\{j \in \mathbb{Z}_+ : t_j \geq \frac{\sigma}{0.9879}\right\} := N < +\infty.$$

Furthermore, $T(e_0, \{t_k\})$ can be estimated by $T(e_0, \{t_k\}) \leq \sigma/0.9879$. Moreover, by Algorithm 3.1 with step length $\iota = 0.01$, one may find the maximum constant $\lambda = 0.09$ satisfying condition (3.10) and the feasible solution

$$P = \begin{pmatrix} 19.4204 & 10.1896 \\ 10.1896 & 189.5647 \end{pmatrix}.$$

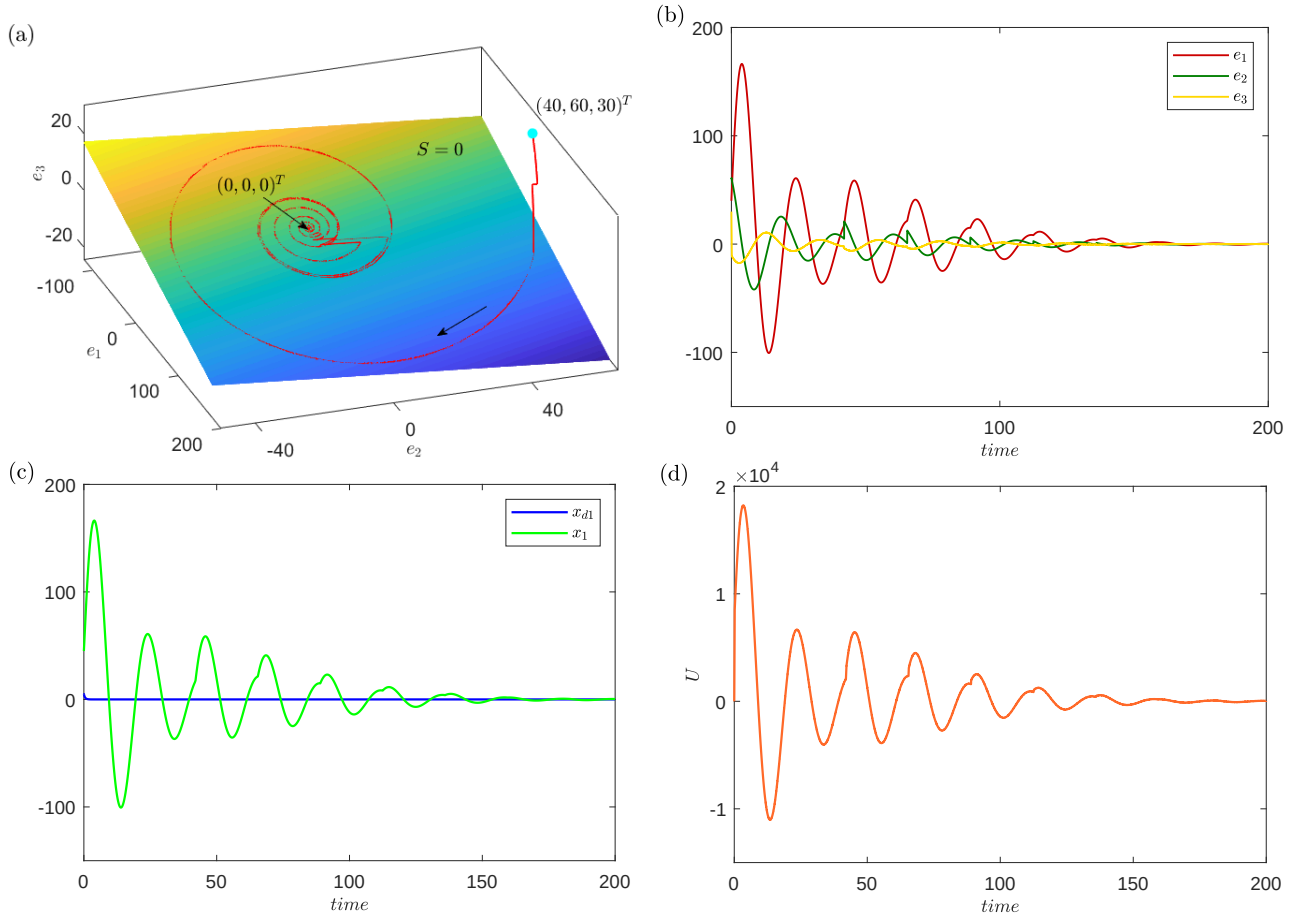

Figure 2. Simulations results with impulse time sequence $\{t_k\}^1$.

It can then be derived from Condition (3.11) the minimum constant $\mu_1 = 8.26$. Based on Theorem 2, the solution of error system (2.7) with $e_0 \in \Omega_\sigma$ can exponentially converge to the origin over the class $\mathcal{S}_2 \subseteq \mathcal{S}_1$ with $\tau > 23.4603$. For simulations, let $x(0) = [45; 65; 35]^T$ and $x_d(0) = [5; 5; 5]^T$. In such case, we choose $\sigma = 41$. The sequence $\{t_k\}$ (denoted by $\{t_k\}^1$) is given by $t_k = \{0.05,\ 42\}$ for $k = 1,\ 2$ and $t_k = 42 + 23.5(k-1)$ for $3 \leq k \in \mathbb{Z}_+$. Figure 2(a),(b) depicts that the solution of error system (2.7).

We get that the states of error system (2.7) with $e_0 \in \Omega_{41}$ can reach $\Gamma(t) = 0$ and then converge to the origin asymptotically. Figure 2(c) shows the positions of the master system (2.6) and the slave system (2.4)–(2.5). The control signal $U(t)$ is depicted in Figure 2(d). Under same condition, if we consider sequence $\{t_k\}$ (denoted by $\{t_k\}^2$) as $t_k = \{0.05,\ 42\}$ for $k = 1,\ 2$ and $t_k = 42 + 13(k-1)$ for all $3 \leq k \in \mathbb{Z}_+$, then it goes against Theorem 2. In this case, it can be seen from Figure 3 that the state of error system (2.7) with $e_0 \in \Omega_{41}$ does not asymptotically converge to the origin, which effectively verifies our obtained results.

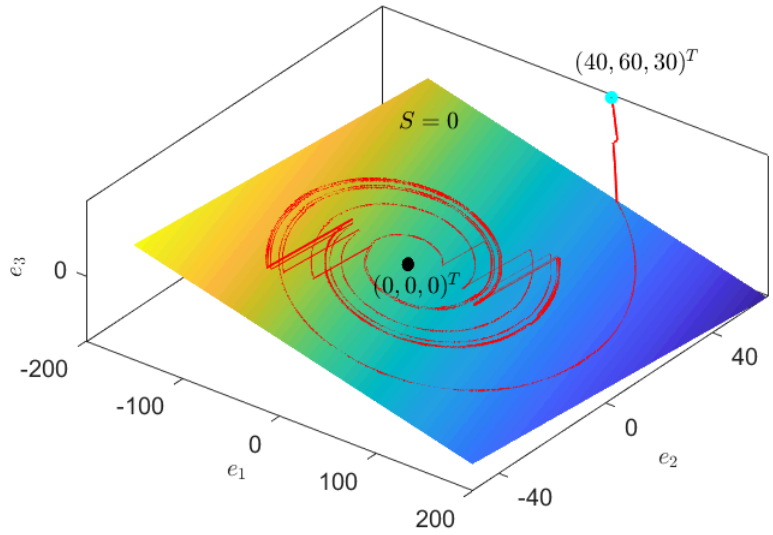

Figure 3. The solution of error system (2.7) with impulse time sequence $\{t_k\}^2$.

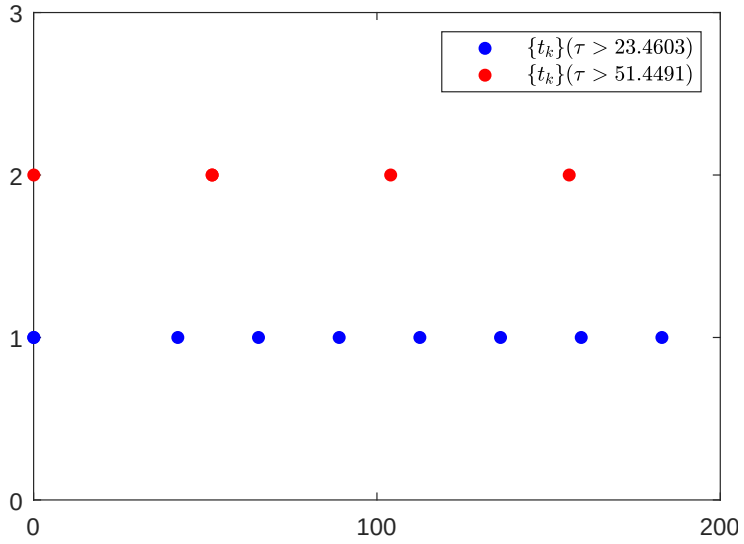

Figure 4. Impulse time sequence $\{t_k\}^2$ and impulse time sequence $\{t_k\}^3$.

In the following, we show the optimality of the selection of the terms λ and μ_1 with the same matrix C. If we choose $\lambda^1 = 0.04 < \lambda$, which goes against Algorithm 3.1, then it can be obtained the minimum

constant $\mu_1^1 = 7.83$. The state of error system (2.7) with $e_0 \in \Omega_\sigma$ can exponentially converge to the origin over the class $\mathcal{S}_2 \subseteq \mathcal{S}_1$ with $\tau_1 > 51.4491$. In simulations, the sequence $\{t_k\}^3$ can be given by $t_k = \{0.05,\ 52\}$ for $k = 1,\ 2$ and $t_k = 52 + 52(k-1)$ for $3 \leq k \in \mathbb{Z}_+$. To illustrate the differences between τ and τ_1 more intuitively, the sequences of $\{t_k\}^2$ and $\{t_k\}^3$ are depicted in Figure 4. It can be observed that, under the premise of guaranteeing stability, the selection of the parameters λ and μ_1 by Algorithm 3.1 relaxes the restriction on the impulsive frequency.

Table 2. Comparison results in estimation of reaching time and convergence performance J.

Method	Estimation of reaching time	Convergence performance J
The proposed SMC in (4.1)	$T(e_0, \{t_k\}) \leq 0.1310$	281.7343
Backstepping control in (4.2)	\	1328

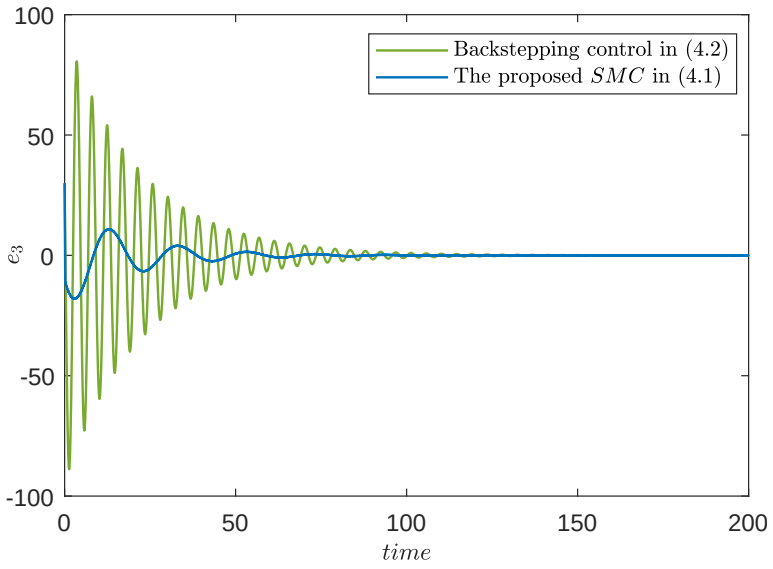

Figure 5. The state trajectories of error system (2.7) under backstepping control in (4.2) and SMC in (4.1).

Next, we compare the proposed SMC with backstepping control. Specifically, suppose that $F_L = 0$ and $g_i = 0$ for $i = 2, 3, 4, 5$. To make fair comparisons, we consider the same initial values $x(0)$, $x_d(0)$ and the convergence rate λ for these two control schemes. In simulations, we choose SMC in (4.1) as the representative for this paper, and the backstepping control for error system (2.7) can be designed by

$$\begin{aligned} U_1(t) &= -\frac{1}{b}\left((a_1 + \lambda + \frac{1}{8}\lambda^3)e_1(t) + (a_2 + 2 + \frac{3}{4}\lambda^2)e_2(t) + (a_3 + \frac{3}{2}\lambda)e_3(t)\right) \\ &= 108.2802e_1(t) + 51.7381e_2(t) + 0.1028e_3(t). \end{aligned} \tag{4.2}$$

Then, the estimation of reaching time and convergence performance J for these two methods are shown in Table 2, where $J := \int_0^T |e_3| ds$. Intuitively, the trajectories of error system (2.7) under the

backstepping control in (4.2) and SMC in (4.1) are depicted in Figure 5. It shows that SMC in (4.1) can enable the system to have a faster convergence speed than backstepping control in (4.2).

5. Conclusions

In the presence of both impulsive disturbance and external disturbances, this article developed a sliding mode control strategy for electrohydraulic position servo systems. Based on linear matrix inequality and average dwell-time approaches, some criteria were presented to ensure the reachability of the sliding surface and the stability of the resulting sliding mode dynamics. Unlike traditional sliding mode control, a relationship between continuous dynamics, impulsive strength, and impulsive frequency was established, which can fully extract the information of impulsive disturbance. It should be noted that the proposed approach requires the impulses to be known or measurable. However, in practical applications, uncertain impulses are unavoidable. In many cases, the impulse signal is neither controllable nor measurable and may even exhibit stochastic characteristics. Thus, the future topic would focus on the electrohydraulic position servo systems subject to uncertain or stochastic impulsive disturbance. In addition, because the linearized model of the electrohydraulic system inevitably introduces approximation errors with respect to the general dynamics with coupled external disturbances, extending the proposed results to more general systems with coupled external disturbances is another interesting topic.

Use of AI tools declaration

The authors declare they have not used artificial intelligence (AI) tools in the creation of this article.

Acknowledgments

This work was supported by the National Key Research and Development Program of China (2023YFC2907504).

Conflict of interest

The authors declare there are no conflicts of interest.

References

1. Y. Chu, X. Han, R. Rakkiyappan, Finite-time lag synchronization for two-layer complex networks with impulsive effects, *Math. Model. Control*, **4** (2024), 71–85. https://doi.org/10.3934/mmc.2024007
2. T. Yang, *Impulsive Control Theory*, Springer, 2002. https://doi.org/10.1007/3-540-47710-1
3. X. He, X. Li, S. Song, Finite-time input-to-state stability of nonlinear impulsive systems, *Automatica*, **135** (2022), 109994. https://doi.org/10.1016/j.automatica.2021.109994
4. Y. He, Y. Bai, Finite-time stability and applications of positive switched linear delayed impulsive systems, *Math. Model. Control*, **4** (2024), 178–194. https://doi.org/10.3934/mmc.2024016

5. W. M. Haddad, V. Chellaboina, S. G. Nersesov, *Impulsive and Hybrid Dynamical Systems: Stability, Dissipativity, and Control*, Princeton University Press, 2006. https://doi.org/10.1515/9781400865246
6. P. Naghshtabrizi, J. P. Hespanha, A. R. Teel, Exponential stability of impulsive systems with application to uncertain sampled-data systems, *Syst. Control Lett.*, **57** (2008), 378–385. https://doi.org/10.1016/j.sysconle.2007.10.009
7. R. Wang, C. Zhang, L. Feng, Z. Wu, Prescribed-time stabilization of uncertain nonlinear impulsive systems with multiple delays, *Electron. Res. Arch.*, **33** (2025), 5207–5230. https://doi.org/10.3934/era.2025233
8. Y. Li, J. Feng, J. Wang, Mean square synchronization for stochastic delayed neural networks via pinning impulsive control, *Electron. Res. Arch.*, **30** (2022), 3172–3192. https://doi.org/10.3934/era.2022161
9. W. Zhou, K. Wang, W. Zhu, Synchronization for discrete coupled fuzzy neural networks with uncertain information via observer-based impulsive control, *Math. Model. Control*, **4** (2024), 17–31. https://doi.org/10.3934/mmc.2024003
10. W. Zhao, K. Li, Y. Shi, Exponential synchronization of neural networks with mixed delays under impulsive control, *Electron. Res. Arch.*, **32** (2024), 5287–5305. https://doi.org/10.3934/era.2024244
11. G. Zheng, Y. Orlov, W. Perruquetti, J. P. Richard, Finite-time-observer design for nonlinear impulsive systems with impact perturbation, *Int. J. Control*, **87** (2014), 2097–2105. https://doi.org/10.1080/00207179.2014.902998
12. J. Liu, X. Liu, W. C. Xie, Input-to-state stability of impulsive and switching hybrid systems with time-delay, *Automatica*, **47** (2011), 899–908. https://doi.org/10.1016/j.automatica.2011.01.061
13. V. Djordjevic, L. Dubonjic, M. M. Morato, D. Pršić, V. Stojanović, Sensor fault estimation for hydraulic servo actuator based on sliding mode observer, *Math. Model. Control*, **2** (2022), 34–43. https://doi.org/10.3934/mmc.2022005
14. Z. Liu, J. Sun, D. Yue, X. Zuo, H. Gao, K. Feng, A review on integral evolution of electro-hydraulic actuation in three momentous domains: Aerospace, engineering machinery, and robotics, in *Fourth International Conference on Mechanical Engineering, Intelligent Manufacturing, and Automation Technology (MEMAT 2023)*, **13082** (2024), 141–159. https://doi.org/10.1117/12.3026210
15. W. Sun, H. Pan, H. Gao, Filter-based adaptive vibration control for active vehicle suspensions with electrohydraulic actuators, *IEEE Trans. Veh. Technol.*, **65** (2015), 4619–4626. https://doi.org/10.1109/TVT.2015.2437455
16. J. Li, L. Kong, H. Liang, W. Li, Review of development and characteristics research on electro-hydraulic servo system, *Recent Pat. Eng.*, **18** (2024), 140–154. https://doi.org/10.2174/1872212118666230711165517
17. X. Yang, H. Chen, J. Mao, Y. Wei, Dynamical behavior of coal shearer traction-swing coupling under corrected loads, *Sci. Rep.*, **10** (2020), 8630. https://doi.org/10.1038/s41598-020-65184-w

18. H. Feng, W. Ma, C. Yin, D. Cao, Trajectory control of electro-hydraulic position servo system using improved pso-pid controller, *Autom. Constr.*, **127** (2021), 103722. https://doi.org/10.1016/j.autcon.2021.103722

19. H. Liu, Y. Li, Y. Zhang, Y. Chen, Z. Song, Z. Wang, et al., Intelligent tuning method of pid parameters based on iterative learning control for atomic force microscopy, *Micron*, **104** (2018), 26–36. https://doi.org/10.1016/j.micron.2017.09.009

20. G. Qiu, Y. Hao, G. Chen, G. Yan, Y. Chen, Prescribed performance trajectory tracking control for electro-hydraulic servo pump-controlled systems with input and state delays, *Machines*, **13** (2025), 1147. https://doi.org/10.3390/machines13121147

21. X. Ren, Q. Guo, T. Li, Initial condition-free prescribed performance fault-tolerant control of electro-hydraulic servo systems with state constraints, *Nonlinear Dyn.*, **113** (2025), 11723–11743. https://doi.org/10.1007/s11071-024-10804-7

22. Y. Zhang, W. Ju, Q. Liu, L. Wei, C. Yin, X. Feng, et al., Control design of the hydraulic support pushing system based on saturation, *Electron. Res. Arch.*, **34** (2026), 336–350. https://doi.org/10.3934/era.2026016

23. G. Mihalev, S. Yordanov, K. Ormandzhiev, H. Stoycheva, T. Todorov, Synthesis of model predictive control for an electrohydraulic servo system using orthonormal functions, in *2024 5th International Conference on Communications, Information, Electronic and Energy Systems (CIEES)*, (2024), 1–6. https://doi.org/10.1109/CIEES62939.2024.10811237

24. G. Shen, Z. Zhu, J. Zhao, W. Zhu, Y. Tang, X. Li, Real-time tracking control of electro-hydraulic force servo systems using offline feedback control and adaptive control, *ISA Trans.*, **67** (2017), 356–370. https://doi.org/10.1016/j.isatra.2016.11.012

25. V. Stojanović, Fault-tolerant control of a hydraulic servo actuator via adaptive dynamic programming, *Math. Model. Control*, **3** (2023), 181–191. https://doi.org/10.3934/mmc.2023016

26. H. Ding, Y. Wang, H. Zhang, Robust output feedback position control of hydraulic support with neural network compensator, in *Actuators*, MDPI, **12** (2023), 263. https://doi.org/10.3390/act12070263

27. Q. Guo, G. Shi, D. Wang, C. He, Neural network–based adaptive composite dynamic surface control for electro-hydraulic system with very low velocity, in *Proceedings of the Institution of Mechanical Engineers, Part I: Journal of Systems and Control Engineering*, **231** (2017), 867–880. https://doi.org/10.1177/0959651817731976

28. C. Wang, J. Wang, Q. Guo, Z. Liu, C. P. Chen, Disturbance observer-based fixed-time event-triggered control for networked electro-hydraulic systems with input saturation, *IEEE Trans. Ind. Electron.*, **72** (2024), 1784–1794. https://doi.org/10.1109/TIE.2024.3429638

29. L. Cheng, Z. C. Zhu, G. Shen, S. Wang, X. Li, Y. Tang, Real-time force tracking control of an electro-hydraulic system using a novel robust adaptive sliding mode controller, *IEEE Access*, **8** (2019), 13315–13328. https://doi.org/10.1109/ACCESS.2019.2895595

30. N. Kumar, K. S. Chaudhary, Position tracking control of nonholonomic mobile robots via H_∞-based adaptive fractional-order sliding mode controller, *Math. Model. Control*, **5** (2025), 121–130. https://doi.org/10.3934/mmc.2025009

31. Z. Mokhtare, M. T. Vu, S. Mobayen, A. Fekih, Design of an lmi-based fuzzy fast terminal sliding mode control approach for uncertain MIMO systems, *Mathematics*, **10** (2022), 1236. https://doi.org/10.3390/math10081236
32. K. Naseri, M. T. Vu, S. Mobayen, A. Najafi, A. Fekih, Design of linear matrix inequality-based adaptive barrier global sliding mode fault tolerant control for uncertain systems with faulty actuators, *Mathematics*, **10** (2022), 2159. https://doi.org/10.3390/math10132159
33. Q. Li, Z. Jin, L. Qiao, A. Du, G. Liu, Distributed optimization of nonlinear singularly perturbed multi-agent systems via a small-gain approach and sliding mode control, *AIMS Math.*, **9** (2024), 20865–20886. https://doi.org/10.3934/math.20241015
34. K. A. Alattas, M. T. Vu, O. Mofid, F. F. El-Sousy, A. K. Alanazi, J. Awrejcewicz, et al., Adaptive nonsingular terminal sliding mode control for performance improvement of perturbed nonlinear systems, *Mathematics*, **10** (2022), 1064. https://doi.org/10.3390/math10071064
35. H. M. Chen, J. C. Renn, J. P. Su, Sliding mode control with varying boundary layers for an electro-hydraulic position servo system, *Int. J. Adv. Manuf. Technol.*, **26** (2005), 117–123. https://doi.org/10.1007/s00170-004-2145-0
36. M. Yang, Q. Zhang, X. Liu, R. Xi, X. Wang, Adaptive sliding mode control of a nonlinear electro-hydraulic servo system for position tracking, *Mechanics*, **25** (2019), 283–290. https://doi.org/10.5755/j01.mech.25.4.22822
37. C. Sun, X. Dong, M. Wang, J. Li, Sliding mode control of electro-hydraulic position servo system based on adaptive reaching law, *Appl. Sci.*, **12** (2022), 6897. https://doi.org/10.3390/app12146897
38. H. Dong, X. Yang, M. V. Basin, Practical tracking of permanent magnet linear motor via logarithmic sliding mode control, *IEEE/ASME Trans. Mechatronics*, **27** (2022), 4112–4121. https://doi.org/10.1109/TMECH.2022.3142175
39. W. H. Chen, X. Deng, W. X. Zheng, Sliding-mode control for linear uncertain systems with impulse effects via switching gains, *IEEE Trans. Autom. Control*, **67** (2021), 2044–2051. https://doi.org/10.1109/TAC.2021.3073099
40. K. Guo, J. Wei, Q. Tian, Nonlinear adaptive position tracking of an electro-hydraulic actuator, *Proc. Inst. Mech. Eng. C*, **229** (2015), 3252–3265. https://doi.org/10.1177/0954406214568821
41. A. K. Behera, B. Bandyopadhyay, X. Yu, Periodic event-triggered sliding mode control, *Automatica*, **96** (2018), 61–72. https://doi.org/10.1016/j.automatica.2018.06.035

AIMS Press